



Surface *p*CO₂ and hydrography in the dense water formation area of the southern Adriatic

- Carlotta Dentico^{1,2}, Angelo Rubino¹, Giuseppe Civitarese², Michele Giani², Giuseppe Siena², Stefano Kuchler²,
 Julien Le Meur², Andrea Corbo² and Vanessa Cardin²
- 6 ¹ Department of Environmental Sciences, Informatics and Statistics, Università Cà Foscari, Venice, Italy
- 7~ 2 National Institute of Oceanography and Applied Geophysics (OGS), Trieste, Italy 8~
- 9 Correspondence to: Carlotta Dentico (cdentico@ogs.it)

Abstract.

5

10

11

12

13

14

15

16

17

18

19

20

21

22

23

24

25

26

27

28

29

30

31

32

33

34

35

36

37

The rising CO₂ concentration in the atmosphere leads to an increase in CO₂ uptake in the ocean and to significant changes in seawater chemistry. These changes, in turn, exert profound effects on marine ecosystems across multiple trophic levels. The Mediterranean Sea is considered a hotspot for climate change. Despite such relevance, observations and studies on its carbonate system remain limited, especially in regions that play a crucial role in regulating air-sea CO2 exchange like intermediate and dense water formation areas. The southern Adriatic Sea, a key site for dense water formation in the eastern Mediterranean, hosts the EMSO ERIC and ICOS ERIC South Adriatic observatory (EMSO-E2M3A), operated by the Italian National Institute of Oceanography and Applied Geophysics (OGS). This facility allows the study of physical and biogeochemical dynamics in the deepest area of the Adriatic Sea. The suite of sensors deployed on the surface buoy allows for the characterization of water mass properties, biogeochemical cycles, dense water formation process, and ocean acidification, particularly in relation to carbon sequestration dynamics. Here, time series of meteorological data (e.g., wind speed, wind direction), sea surface physical parameters (e.g., temperature, salinity), dissolved oxygen and partial pressure of CO₂ (pCO_{2sw}) and pH from 2014 to 2024 will be presented (https://doi.org/10.13120/y2hw-1j63, Cardin et al., 2025). In particular, quality check and correction and post-processing methods applied to the data will be discussed. The validated surface dataset provides a consistent pCO_{2sw} time series for the Adriatic Sea, with values and seasonal variability in agreement with previous observations across the Mediterranean. Associated temperature, salinity, oxygen, and wind measurements reproduce expected regional patterns, confirming the robustness and suitability of the presented dataset for further biogeochemical and climate-related analyses.

1. Introduction

The concentration of CO_2 in the atmosphere has rapidly increased from around 280 parts per million (ppm) at the beginning of the Industrial Revolution in 1750, to 427 ppm in February 2025 (http://co2.earth/). This increase is the primary driver of the intensification of the ocean CO_2 sink, which has increased from 1.2 ± 0.4 GtC yr¹ in the 1960s to 2.9 ± 0.4 GtC yr¹ in the period 2014 - 2023 (Friedlingstein et al., 2025). However, the net air-sea CO_2 flux is a highly dynamic process exhibiting significant spatial and temporal heterogeneity driven by complex natural and anthropogenic processes (Takahashi et al., 2009; Friedlingstein et al., 2025).





39 as ocean acidification (OA). These changes are associated with a reduction in seawater pH and carbonate ion 40 concentrations, and an increase in dissolved CO2, dissolved inorganic carbon and bicarbonate ions (Orr et al., 41 2015). OA poses a significant threat to marine ecological communities (e.g., Gattuso and Hansson, 2011; Riebesell 42 et al., 2013; IPCC, 2021), which rely on specific ranges of key carbonate chemistry parameters for their survival. 43 Continuous, high-quality ocean carbon data are therefore essential to monitor these changes, predict future 44 impacts, and contribute to the biogeochemical Essential Ocean Variables (EOVs) framework of the Global Ocean 45 Observing System (GOOS). 46 The Mediterranean Sea is a recognized climate change hotspot. The unique hydrological and biogeochemical 47 characteristics of the Mediterranean Sea water (Alvarez et al., 2023) enhance the uptake and transfer of CO₂ to 48 depth more efficiently than the global ocean (Schneider et al., 2010; Hassoun et al., 2015), with anthropogenic 49 CO₂ having already penetrated all major water masses of the basin (Touratier and Goyet, 2011; Hassoun et al., 50 2015; Ingrosso et al., 2017). Research has shown that the Mediterranean Sea is already experiencing negative pH 51 trends (e.g., Hassoun et al., 2015; Kapsenberg et al., 2016; Cantoni et al., 2024; Garcia-Ibanez et al., 2024), often 52 with a wider range than those observed in the Atlantic Ocean. However, reliable biochemical and biological 53 carbonate system data remain limited (Hassoun et al. 2022), and comprehensive OA data are still sparse, not easily 54 accessible and often not scalable. Within the Mediterranean, the southern Adriatic Sea is a particularly critical 55 region, serving as the primary site for dense water formation in the eastern Mediterranean (Robinson et al., 2001). 56 About 82% of the Adriatic Dense Water (AdDW) is formed by winter convection (Ingrosso et al., 2017), while 57 the remaining part has its origin on the northern Adriatic shelf and in the middle Adriatic (Ovchinnikov et al., 58 1985; Bignami et al., 1990; Malanotte-Rizzoli, 1991). The Northern Adriatic Dense Water (NAdDW) is formed 59 in winter, due to the cooling of the entire water column caused by E-NE wind (named Bora). Winter convection 60 and intense Bora winds produce the densest (potential density anomaly, $\sigma_{\theta} = 29.2 \text{ kg m}^{-3}$) water mass in the 61 Mediterranean Sea (Malanotte-Rizzoli, 1991; Artegiani et al., 1997). These meteorological and oceanographic 62 conditions which favour the heat loss, can also favour CO2 dissolution when surface water is undersaturated with 63 respect to the overlying atmosphere. The NAdDW is partially collected in the middle Adriatic and partly flows 64 southward to the deepest part of the southern Adriatic, ventilating the deep southern Adriatic Pit (Cardin et al., 65 2011; Le Meur et al., 2025). 66 The physical and biogeochemical properties of the southern Adriatic Sea are monitored through coordinated open-67 ocean observations, including research vessels, moorings, and autonomous platforms such as ocean gliders and 68 Argo floats. Here, meteorological, physical and biogeochemical data collected by the EMSO ERIC and ICOS 69 ERIC South Adriatic observatory named EMSO-E2M3A, operated by the Italian National Institute of 70 Oceanography and Applied Geophysics (OGS) will be presented. The observatory is part of the European 71 Multidisciplinary Seafloor and Water Column (EMSO) - South Adriatic Regional Facility - (EMSO ERIC) and 72 of the Integrated Carbon Observation System (ICOS) networks. EMSO-E2M3A has been in operation since 2006 73 representing the longest open-ocean time series in the whole Adriatic being an ideal site for the investigations of 74 several physical (Bensi et al., 2013, 2014; Cardin et al., 2020; Amorim et al., 2024; Le Meur et al., 2025) and 75 biogeochemical processes (Ingrosso et al., 2017) in the whole water column, as well as air-sea interactions. The 76 time series presented here, represent an important resource to understand physical and biogeochemical changes 77 occurring in the region, the OA and the biological responses of planktonic organisms, and to evaluate

This accelerated oceanic CO₂ uptake is the direct cause of changes in seawater chemistry commonly referred to





82

83

84

85

86

87

88

89

90

91

92

93

94

95

96

97

98

99

100

101

102

103

104

105

106

107

108

109

110



biogeochemical model performance. A potential use of this time series will also be discussed, in particular related to the calculation of sea-air CO₂ flux and the associated uncertainties. These results will contribute to assess the role of the southern Adriatic in regulating CO₂ exchange and to quantify the carbon stored in the deep layers.

2. Material and methods

2.1. Study area

The southern Adriatic (SAd) is the deepest part of the Adriatic Sea, with the southern Adriatic Pit (SAP) reaching maximum depths of approximately 1250 m (Figure 1a). This area is featured by a quasi-permanent cyclonic circulation, and dense water formation takes place at the centre of the gyre through winter open-ocean convection (Ovchinnikov et al., 1985; Gačić et al., 1997) contributing to the eastern Mediterranean thermohaline circulation (Robinson et al., 2001). Different water masses can be distinguished in the SAd: i) the Adriatic Surface Water (AdSW) is a relatively fresh and warm water mass, which originates from the Po River runoff and flows southward along a narrow coastal layer of the western Italian shelf and exits through the Strait of Otranto; ii) Ionian Surface Water (ISW), entering the basin in the eastern part of the Otranto Strait can be found in the upper part of the water column; iii) the Levantine Intermediate Water (LIW), which usually enters in the Adriatic at depths between 200 m and 600 m and it is characterised by high salinity between 38.75 and 39.00 (Vilibić and Orlić, 2001; Fedele et al., 2021; Taillandier et al., 2022). The source of the LIW is the Levantine basin, from where its salinity, temperature, and dissolved oxygen decrease on their way toward the Adriatic Sea; and iv) the Adriatic Deep Water (AdDW), which represents one of the main component of deep waters for the whole Eastern Mediterranean basin (Schlitzer et al., 1991; Roether and Schlitzer, 1991; Schroeder et al., 2024), and occupies the bottom layer of the SAP. The hydrological and biogeochemical dynamics of the SAd are strictly linked to that of the Ionian Sea (IS) by means of the Bimodal Oscillating System (BiOS) that changes the circulation of the North Ionian Gyre (NIG) from cyclonic to anticyclonic and vice versa, on decadal time scale (Gačić et al., 2011; Civitarese et al., 2023). The reversal of the NIG led to the entrance of the Atlantic Water (anticyclonic NIG), which decreased the salinity and the density of the AdDW, or of the warm and salty Levantine Intermediate Water and Levantine Surface Water (cyclonic NIG). This latter results in an increase in the salinity (and density) of the outflowing AdDW into the IS that gradually impairs the cyclonic NIG, eventually reversing it to an anticyclone. The physical and biogeochemical data presented here were measured by surface sensors deployed at the EMSO-E2M3A regional facility. The site is located in the center of the SAP (nominal position 41.5053°N, 18.0806°E; Figure 1a) and it is composed of two independent mooring lines (Figure 1b). The primary mooring line hosts a surface buoy allowing real-time data transmission of meteorological data, ocean surface hydrological and biogeochemical data. The secondary mooring is composed of an array of sensors positioned at several depths aimed at measuring physical and biogeochemical parameters, from the seafloor to the upper layer. Further information on the site can be found in Bozzano et al. (2013) and Ravaioli et al. (2016).



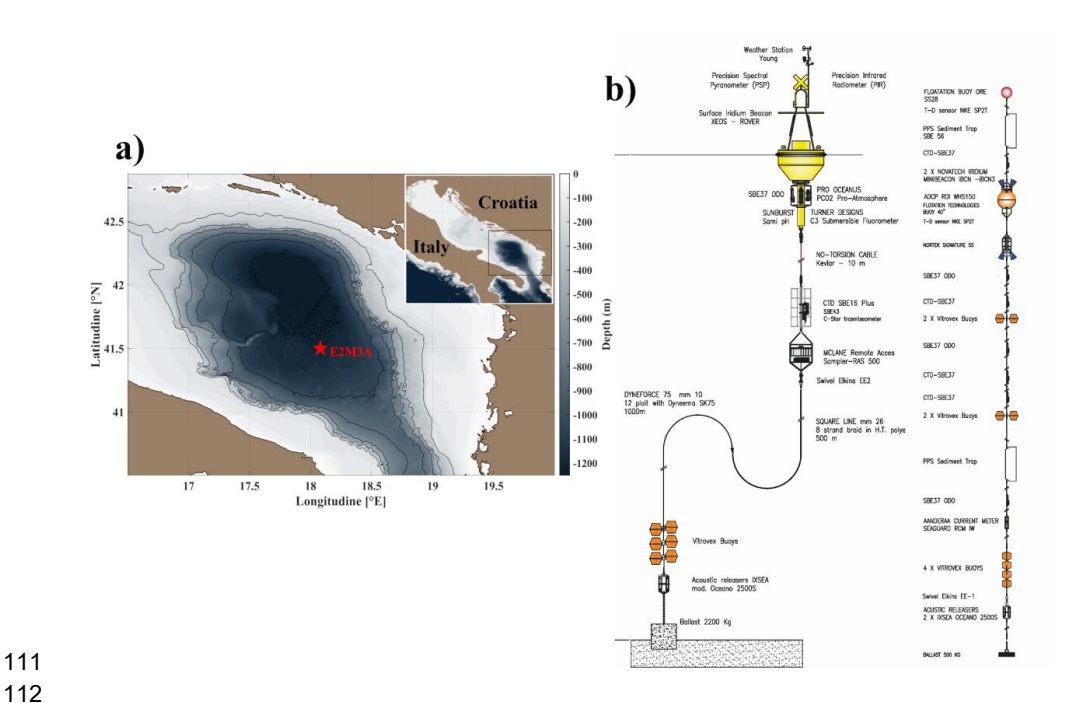


Figure 1. a) Map of the study area with the location of EMSO-E2M3A station (nominal position 41.5053°N, 18.0806°E) represented by the red star, moored in the South Adriatic Pit, and b) scheme of the surface buoy and of the deep mooring.

2.2. Data collection and quality check

Time series from autonomous sensors at key locations are fundamental components of the GOOS (https://www.ioc.unesco.org/). They provide a continuous view of the temporal behaviour of the system on long-term baselines, enabling the measurement of a wide range of interrelated variables, promoting the sharing of data, as demonstrated by international initiatives such as MonGOOS (The Mediterranean Oceanographic Network for the Global Ocean Observing System), OceanSITES and FixO3 (Fixed point Open Ocean Observatory network, FP7 EUProject). Nevertheless, the data acquired by sensors on ocean observing infrastructures, requires quality controls according to defined standards to serve as reliable reference points. In the next sections, a detailed description of the data quality procedures applied to the data will be discussed.

2.2.1. Meteorological data

Meteorological high-frequency (hourly) data were collected by Young (R.M. Young Company) sensors on the meteorological station located on the surface buoy. This data includes: air temperature (°C), wind speed (m/s), wind gust (m/s), wind direction (°deg), air pressure (hPa), relative humidity (%) and long and short wave radiation (W/m²). Horizontal wind speed and direction have been measured by a Wind Monitor-MA (model 05106), with accuracy of \pm 0.3 m/s and \pm 3 degrees respectively, pressure is measured by a barometric pressure sensor (model 61402V) with digital accuracy of 0.2 hPa (at 25°C) and 0.3 hPa (-40°C to +60°C) and analog accuracy of 0.05% of analog pressure range, and relative humidity and air temperature were measured by a Relative Humidity/Temperature Probe (model 41382VC) with accuracy equals to \pm 0.1% (at 23°C) and \pm 0.3°C (at 23°C)





respectively. Data have been corrected and quality controlled following the procedure described in Cardin et al. (2014). This procedure consists of a series of tests on the data to identify erroneous and anomalous values to establish if the data have been corrupted. Checks on individual or consecutive data points provide information for instrument errors, and checks on regional ranges, consistency with physical limits of the data (spikes), rate of change, and stationarity of data were also performed. No editing of invalid data and replacement of missing data are performed, but only a flag is given to the data at each of the automatic quality control checks.

2.2.2. CTD data

139

140

141

142

143

144

145

146

147

148

149

150

151

152

153

154

155

156

157

158

159

160

161

162

163

164

165

166

167

168

169

170

171

Temperature (Temp, °C), salinity (Sal) and dissolved oxygen (DO, µmol/kg) high-frequency data (hourly) were collected by a CTD (Conductivity-Temperature-Depth) SeaBird SBE 37-ODO probe at 2 m depth. The SBE 37-ODO is a high-accuracy conductivity and temperature recorder that includes an Optical Dissolved Oxygen (DO) sensor (SBE63). The instrument has an accuracy of \pm 0.002 °C, \pm 0.003 mS/cm and \pm 0.1% of full scale, for temperature, conductivity and oxygen respectively. The data underwent an initial quality control as described in Cardin et al. (2014). First, a physical range test is applied to the data to control the physical significance of each parameter. Given the general increase in salinity in the SAP, as reported by Amorim et al. (2024) and Le Meur et al. (2025), a modified threshold for salinity than Cardin et al., (2014) was applied. Despiking was then performed to highlight the values having a difference with neighbouring values greater than the defined threshold. Finally, a rate of change test was performed as the final step of the initial quality control procedure. While despiking identifies isolated outliers that differ significantly from the neighbouring values, the rate of change identifies fluctuations that are too rapid. After this step, linear interpolation was applied to data gaps greater than 6 hours. While the first quality control consisted of statistical analyses, the second quality control procedure focuses on the comparison between SBE 37-ODO time series and reference data collected during oceanographic cruises. For temperature and conductivity (salinity), fourteen corrected CTD casts performed near EMSO-E2M3A from 02/11/2015 to 31/10/2024 were used. The CTD casts were corrected according to the post-processing methods suggested by the manufacturer (SeaBird software). These CTD casts were taken as reference as they have a higher accuracy and higher vertical resolution than the data measured by the SBE 37-ODO. The time series were compared with the reference CTD casts to detect any offset, which t, if present, was added to the time series. Another type of error that can affect a time series and needs to be corrected is the drift of the instrument. Particular attention should be paid to the natural variability and trend of the different variables characterizing the dynamics occurring in the area. In this case, the drift was calculated considering both short time periods, and the entire time span of the SBE 37-ODO time series. Calculating the drift only over a short time scale, that may result from an episodic physical process, is not representative of the long-term natural trend. DO (μmol/kg) data were quality checked by comparing the probe data with DO (µmol/kg) from discrete samples collected at the EMSO-E2M3A station. Samples for the determination of DO were collected in calibrated 50 ml bottles and DO was determined by the Winkler potentiometric titration method (Oudot et al., 1988). The precision of the measurements was evaluated on three to five replicates collected from the same Niskin bottle, and was, on average, 0.08%. Before the comparison with reference seawater samples, post-processing of DO data follows the same quality control procedures applied to temperature and conductivity (salinity). However, an additional quality control step for DO was introduced before the second quality control to account for the adjustment time of the oxygen sensor at switch-on. It consisted of fitting a double exponential function and flagging initial values that deviated





172 significantly from the long-term behavior. The comparison was possible with a limited number of samples, which

173 revealed a mean difference between DO from discrete samples and DO measured by the probe of -9.36 μmol/kg

174 (-0.21 mL/L). Further information on the correction methods applied can be found in Bensi et al., (2012, 2014),

175 Cardin et al. (2020), Amorim et al., (2024) and Le Meur et al., (2025).

2.2.3. Sea surface pCO₂

177 Since 2014, a Pro-Oceanus CO₂-Pro sensor has provided high-frequency (every 4 hours) autonomous 178 measurements of *p*CO₂ in water (*p*CO_{2sw}, μatm) at a depth of approximately 2 meters. In 2023, a Pro-Oceanus 179 CO₂-Pro ATM sensor was deployed, allowing high-frequency (every 4 hours) continuous measurements of 180 *p*CO_{2sw} and atmospheric *p*CO₂ (*p*CO_{2atm}, μatm) in alternately mode. Pro-Oceanus CO₂ sensors measure dissolved 181 CO₂ with a semi-permeable membrane, allowing CO₂ in the gas phase to equilibrate with the surrounding water. 182 The 'wet' CO₂ concentration (xCO₂, ppmv) is then detected by an infrared sensor, and the *p*CO_{2sw} (in μamt) is 183 calculated by multiplying this concentration by the total pressure, in millibars (mbar), within the instrument's gas 184 stream:

185 186

176

$$pCO_{2sw} = xCO_2 x \frac{P}{1013.25}$$
 (1)

187 188

189

190

191

192

193

194

195

196

197

198

199

200

201

202

203

204

Long-term signal stability of the data is achieved by an automatic zero compensation function that removes CO2 from the system at regular intervals and records a new CO2 baseline value. Both sensors (CO2-Pro and CO2-Pro ATM) have an accuracy of ± 5 μatm. As the first step in the data quality control procedure, the auto-calibration values following the automatic zero adjustment were discarded. If no stability of the measurements was detected, also the second and, in some cases, the third values after the automatic zero were removed. In addition, outliers resulting from sensor malfunctions or maintenance operations were removed. Calibration by vendors and pre and post deployment checks of the sensors were regularly performed at the in-house laboratory at OGS, the Calibration and Metrology Center (CTMO), to ensure the quality of the measurements presented here. Additionally, reference water samples of pH and total alkalinity were collected near the sensor for the calculation of pCO_{2sw}. Calculations were performed using the CO2SYS software (Pierrot et al., 2006) with the carbonic acid equilibrium constants (K1 and K2) from Lueker et al. (2000), the dissociation constant for HSO₄ from Dickson et al. (1990) and the borate dissociation constant from Lee et al. (2010). The pCO_{2sw} from discrete samples ($pCO_{2sw(@sample}, \mu atm)$ was matched with the closest hourly pCO_{2sw} from sensor (pCO_{2sw@probe}, μatm) resulting in the comparison of seven data in the period 2015 - 2024 (Table 1). When matching within this short time interval was not possible, a comparison between the pCO_{2sw@sample} and the pCO_{2sw@probe} with a difference of a few days (no more than one week) was performed. To ensure comparability, $pCO_{2sw@probe}$ was adjusted to the temperature measured at the time of seawater sampling, which was also used for the determination of pCO_{2sw@probe}, according to Takahashi et al., (1993):

205 206

207
$$pCO_{2sw@Tadj} = pCO_{2sw@probe} x exp^{(0.0423 x (T_{probe} - T_{sample})}$$
 (2)

208



where $pCO_{2sw@Tadj}$ (µatm) is the pCO_{2sw} probe value adjusted for the temperature difference, $pCO_{2sw@probe}$ is the pCO_{2sw} measured by the probe (µatm), T_{probe} is the temperature (°C) measured by the SeaBird SBE 37-ODO during the acquisition of the $pCO_{2sw@probe}$ and T_{sample} is the temperature (°C) measured by the CTD casts during the collection of the discrete samples.

213214215

216

209

210

211

212

Table 1. Comparison between pCO_{2sw} from discrete samples ($pCO_{2sw@sample}$, μ atm) and pCO_{2sw} from probe ($pCO_{2sw@probe}$, μ atm). The difference is calculated as $pCO_{2sw@sample}$ - $pCO_{2sw@probe}$.

Date	pCO _{2sw@samples} (μatm)	pCO _{2sw@probe} (μatm)	Difference (µatm)	
20/10/2014	328.11	361.23	-33.12	
29/10/2015	381.46	382.63	-1.17	
29/07/2017	486.74	480.40	6.34	
08/10/2018	381.26	397.50	-16.34	
19/10/2019	399.33	379.15	20.18	
30/10/2022	383.45	420.90	-37.45	
05/12/2023	361.00	364.64	-3.64	

217 218

219

220

221

222

223

224

225

226

227

228

229

230

231

232

233

234

235

236

237

238

In three out of seven cases, the accuracy of the measurements falls within either the manufacturer's stated accuracy (±5 μatm) or the target accuracy defined by the ICOS network for Fixed Ocean Stations (±10 μatm, https://www.icos-otc.org/). In all other cases, these criteria were not met. However, during the recent ICOS Ocean Thematic Centre (OTC) pCO₂ inter-comparison experiment (Steinhoff et al., 2025), it was demonstrated that deviations of around 15 - 20 µatm can be expected by membrane sensors, particularly under conditions of increasing temperature. Additionally, in the two cases of very high deviation, biofouling-likely developing during the spring/summer period could be identified as a probable contributing factor for this difference. Indeed continuous monitoring and maintenance of open ocean fixed observatories is often constrained by available infrastructure, and strict ship time windows influenced by several factors such as weather conditions (Coppola et al., 2016). Additionally, in 2020, pCO_{2sw} measurements were acquired by two Unmanned Surface Vehicles (USVs) from Saildrone Inc. (USA) during the ATL2MED demonstration experiment around the EMSO-E2M3A observatory (Martellucci et al., 2024a; 2025). One of the saildrone was equipped with an ASVCO2 system developed by PMEL (NOAA's Pacific Marine Environmental Laboratory). This system fed seawater in a bubble equilibrator (Friederich et al., 1995), and the partially dried xCO₂ is measured with an infrared detector (LI-COR 820 CO2 gas analyser). A two-point calibration was used, where the first is a reference gas from NOAA/ESRL, while the second is air purged for CO₂. Detailed description of the correction, adjustment and quality of pCO_{2sw} Saildrone data can be found in Martellucci et al. (2024a). A similar trend (significant correlation coefficient of 0.77, p-value < 0.01) and a constant offset of 16 µatm between the Saildrone and EMSO-E2M3A data were reported, providing an additional line of evidence for the reliability of this dataset.

Due to the limited number of reference water samples and their incomplete representation of the full CO_2 annual cycle, no corrections to the pCO_{2sw} data were applied.



240

241

242

243

244

245

246

247

248

249

250

251

252

253

254

255

256

257

258

259

260

261

262

263

264

265

266

267

268

269

270

271

272

273

274

275

276



2.2.4. pH data

Hourly pH data were obtained from a SAMI-pH sensor deployed at a depth of 2 meters, covering a two-year period from 2015 to 2016. The instrument uses a high-accuracy colorimetric method, in which seawater is pumped through the sensor and mixed with a pH-sensitive indicator solution (meta-Cresol Purple). According to certified reference material (CRM) intercomparisons, the sensor provides an accuracy of ± 0.003 pH units and a precision of about 0.001 pH units. Calibration by vendors and pre deployment checks of the sensor were performed by the OGS CTMO facility. Discrete samples in the region were also collected in 2015, but no cruises were conducted in the region in 2016. Water samples for validation were collected in 250 mL borosilicate bottles and preserved with mercury chloride (HgCl₂) to prevent biological activity. Samples were stored in the dark and kept cool until laboratory analysis at the OGS facilities. Total scale pH (pH_T) was determined spectrophotometrically following the standard operating procedure SOP 6b described in Dickson et al. (2007). Analyses were performed using a Cary 100 Scan UV-Visible spectrophotometer with a 10 cm pathlength cylindrical quartz cell and a purified 4 mM m-Cresol Purple indicator dye. Prior to measurement, samples were equilibrated to 25°C, then subsampled by siphoning through a Tygon tube to avoid gas exchange, ensuring no headspace was present in the cuvette. pH_T was measured immediately after sub-sampling. The precision of the measurements was evaluated on three to five replicates collected from the same Niskin bottle, and was, on average, 0.01%. During the analysis, the temperature of the samples was controlled using a thermostatic cell holders inside the spectrophotometer, connected to a circulation criothermostat (LAUDA RE415) and monitored with a digital thermometer (VWR Traceable). The mean difference between the three discrete samples and the probe measurements was equal to -0.05 pH units. No further correction to the time series was applied.

3. Robustness and seasonal consistency of the dataset

The surface dataset presented here has been carefully corrected and validated, as described in the previous sections, and all data are publicly available (https://doi.org/10.13120/y2hw-1j63, Cardin et al., 2025). The resulting pCO_{2sw} time series (Figure 2a) falls within the expected range of variability for the region. Both the values and seasonal amplitudes are consistent with previous observations in different regions of the Mediterranean Sea (e.g., Pecci et al., 2024; Garcia-Ibañez et al., 2024; Frangoulis et al., 2024) and in the Adriatic Sea (e.g., Turk et al., 2010; Cantoni et al., 2012; Ingrosso et al., 2016; Urbini et al., 2020; Cantoni et al., 2024). Lower values are observed in winter with pCO_{2sw} concentrations between 350 μatm and 400 μatm, largely due to cooling and vertical mixing that enhance CO₂ solubility. In contrast, summer values exceed 500 μatm, and occasionally rise above 550 µatm, closely following surface warming and stratification. Alongside pCO_{2sw}, other physical and biogeochemical parameters measured at the site further describe the surface layer dynamics. Temperature reflects the seasonal alternation between winter mixing and summer stratification, with values ranging from 14 °C in winter to 28 °C in summer (Figure 2b). Surface temperatures appear slightly higher than those reported for the northwestern Mediterranean, especially in summer. Marked interannual variability characterizes salinity (Figure 2c), with maximum values exceeding 39 in several years (for instance in 2017, 2020, 2021 and 2022) consistent with previously reported values in the SAP (e.g., Mihanović et al., 2021; Menna et al., 2022). These salinity values are typically higher than those observed in the central Mediterranean (e.g., Pecci et al., 2024) or the northwestern Mediterranean (Garcia-Ibañez et al., 2024) reflecting the influence of warm, saline waters of Levantine/Cretan



283 284

285

origin entering the area (see Sect. 2.1). Oxygen concentrations follow the expected seasonal dynamics (Figure 2d): higher during winter mixing, when ventilation dominates, and lower during the productive season, when biological activity consumes oxygen (e.g., Martellucci et al., 2024b). Wind data (Figure 2e) are also consistent with the regional climatology (e.g., Turk et al., 2010; Pecci et al., 2024), and underline the role of atmospheric forcing in sustaining vertical exchanges, particularly in winter.

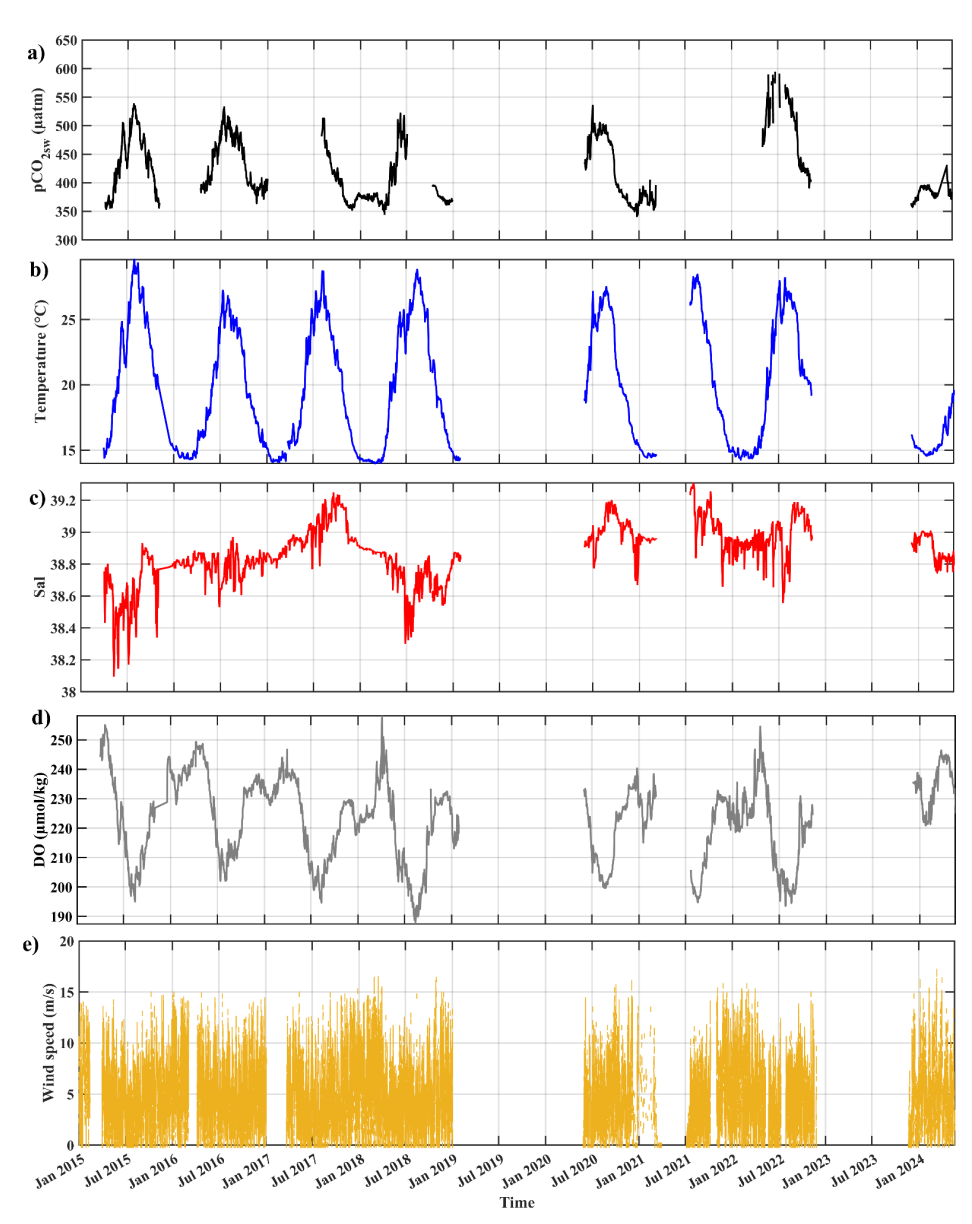


Figure 2. Time series of sea surface a) partial pressure of CO2 (pCO2sw in μ atm); b) Temperature ($^{\circ}$ C); c) Salinity (Sal); d) dissolved oxygen (DO in μ mol/kg); and e) Wind speed (m/s). The variables were measured in the period 2015 - 2024 at EMSO-





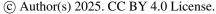
 E2M3A observatory. Periods of missing data were due to maintenance operations, malfunctioning of the sensors and/or the removal of measurements that failed the quality-control procedures described in Sect. 2.2.

A summary of the main biogeochemical and hydrographic variability reported in other Mediterranean regions from fixed ocean stations in the recent year is provided in Table 2.

Table 2. Summary of pCO_{2sw} and hydrographic variability in other oceanographic regions of the Mediterranean sea.

Observational site	Time span	pCO _{2sw}	Hydrography	Dissolved oxygen	Wind speed	References
Lampedusa Oceanographic Observatory (Central Mediterranean sea)	December 2021 - June 2023	Seasonal variability: 350 µatm (winter) and 525 µatm (summer)	Salinity ranges: 36.9 - 38.2 Sea surface temperature ranges: 16°C (winter) and 29°C (summer)	,	Wind speed ranges: between 0 m/s and 15 m/s	Pecci et al., 2024
L'Estartit Oceanographic Station and the Blanes Bay Microbial Observatory (Northwestern Mediterranean Sea)	January 2010 - August 2019	Seasonal variability (fCO ₂): 350 µatm (winter) and 500 µatm (summer)	Salinity ranges: no clear seasonal cycle, values around 37.9 ± 0.3 Sea surface temperature ranges: 13°C (winter) and 23°C (summer)		-	Garcia-Ibañez et al., 2024
POSEIDON fixed platform (Eastern Mediterranean Sea)	January 2020 - May 2023	Seasonal variability: 350 µatm (winter) and ~500 µatm (summer)	Salinity ranges: 39 - 39.6 Sea surface temperature ranges: 15.3°C (winter) and 28.3°C (summer)	,	,	Frangoulis et al., 2024
Gulf of Trieste (Northern Adriatic Sea)	2007-2008; 2008 - 2009; 2011-2013; 2014-2017	Seasonal variability: 220 µatm (winter) and between 475 µatm and 500 µatm (summer)	Salinity ranges: 36 - 37.5 but strong influence of rivers (values < 36) Sea surface temperature ranges: 8°C (winter) and between 26 and 29.5°C (summer)	Dissolved oxygen range: 270 µmol/kg (winter) and around 200 µmol/kg (summer)	Wind speed ranges: between 0 m/s and 15 m/s	Turk et al., 2010; Cantoni et al., 2012; Ingrosso et al., 2016; Urbini et al., 2020; Cantoni et al., 2024

Overall, the consistency of seasonal and interannual patterns, and their alignment with well-known physical and biogeochemical drivers such as convection, stratification, and biological activity, strongly support the reliability of the dataset. These results reinforce the robustness of the observations and provide a solid basis for further scientific interpretation.





299

300

301

302

303

304

305

306

307

308

309

310

311

312



4. Extended and potential future applications of the dataset: calculation of atmospheric carbon flux (FCO₂)

The dataset presented here can be used to describe physical and biogeochemical properties of surface water in the SAP, as well as to estimate the atmospheric carbon flux (FCO₂). This is essential for evaluating the role of the SAP as a potential carbon source or sink across various temporal scales. Ensuring the reliability of air–sea CO_2 flux calculations requires careful evaluation of atmospheric pCO_2 and wind speed data, as different parameterizations may need to be applied and some input data recalculated to meet the requirements of the FCO_2 formulation. In particular, different parameterizations of the gas transfer velocity could yield divergent results. Equally important is the quality of pCO_{2sw} data from sensors. As reported in Steinhoff et al. (2025), it is essential to have a certain degree of knowledge and expertise to produce and interpret optimal quality data, especially for membrane-based systems (such as the submersible Pro-Oceanus sensors) that are easier to operate in the field but require critical understanding of the instrument's characteristics for data processing. Careful validation and quality control of these input parameters are therefore essential. Addressing these methodological considerations is a prerequisite for producing credible flux estimates and, ultimately, for advancing the understanding of carbon dynamics in the SAP.

5. Data availability

- Data described in this work are freely available at the National Oceanographic Data Center (NODC) of the
 National Institute of Oceanography and Applied Geophysics (https://doi.org/10.13120/y2hw-1j63, Cardin et al.,
- 315 2025).

316

317

318

319

320

321

322

323

324

325

326

327

328

329

330

331

332

333

334

6. Conclusions

High frequency observations from fixed stations, such as surface buoys and/or moorings, play a crucial role in assessing the regional variability of the carbon cycle in the Mediterranean Sea across different time scales. The dataset presented here provides a comprehensive resource for exploring the biogeochemical and physical dynamics of the sea surface in the dense water formation area of the southern Adriatic. For the first time, highfrequency observations of meteorological, hydrographic and seawater pCO2 and pH data are presented. In addition, the methods used to perform quality control of the data and possible improvements are discussed. This latter is particularly important for pCO_{2sw} data as many challenges (such as strict ship time windows) were faced in the region as discussed in Sect. 2.2.1. Nevertheless, the dataset presented here offers valuable resources for characterising regional CO₂ dynamics, especially given the limited observational coverage of the area. Making this time series available for the first time is a significant advancement, particularly considering the strategic importance of the region as a key dense water formation area and for air-sea interaction which are fundamental mechanisms for the capture and storage of atmospheric CO₂. Thus, this dataset provides a valuable example for estimating local surface hydrological and biogeochemical dynamics based on high-resolution regional observations with a high degree of accuracy. This dataset could be also used to characterize carbon flux in the SAP using only in situ observations, taking into account the considerations discussed in Sect. 4 and providing explicit estimates of uncertainties associated with CO2 flux calculations. In particular, it includes key parameters such as atmospheric pCO2 and wind speed, which are typically derived from other observatories or retrieved from





models. However, some of the data (*p*CO_{2atm}) currently cover only limited time periods, making data integration necessary to ensure consistency in flux estimates.

337 338

339

340

341

342

343

344

345

Author contribution.

CD: data curation, investigation, validation, writing (original draft), writing (review and editing), conceptualisation, formal analysis, software. AR: investigation, writing (review and editing), conceptualisation. GCi: data curation, investigation, validation, writing (review and editing), conceptualisation. MG: data curation, investigation, validation, writing (review and editing), conceptualisation. GCo: investigation, writing (review and editing), conceptualisation, writing (review and editing), validation, software. SK: data curation, writing (review and editing), validation, writing (review and editing), software. VC: funding acquisition, project administration, data curation, investigation, validation, writing (review and editing), conceptualisation, supervision.

346 347 348

Competing interests. The contact author has declared that none of the authors has any competing interests.

349 350

Acknowledgement.

351 This work benefited from access to E2M3A South Adriatic Regional facility, an EMSO-IT/ICOS-IT and EMSO-352 ERIC and ICOS Site, operated by OGS. Dataset and activities were partially funded by EMSO Italian Joint 353 Research Unit, by OGS and by the EU - Next Generation EU Mission 4, Component 2, Investment 3.1, "Fund for 354 the realisation of an integrated system of research and innovation infrastructures," for Project IR0000032 -355 ITINERIS - Italian Integrated Environmental Research Infrastructures System. The authors express their gratitude 356 to the PHYS, BIO and TEC teams, as well as the CTMO units of OGS and to the CNR-ISP, for their essential 357 contributions and continuous efforts in operating and maintaining the EMSO/ICOS-E2M3A regional facility. The 358 authors thank Christian Puntini for his valuable contribution to curating the meteorological data. The author also 359 acknowledges the creators of ChatGPT, used to improve the English writing in some parts of this manuscript.

360

361

References

- 362 Alvarez, M., Catala, S.T., Civitarese, G., Coppola, L., Hassoun, A., Ibello, V., Lazzari, P., Lefevre, D., Macias,
- 363 D., Santinelli, C., and Ulse, C.: Mediterranean Sea general biogeochemistry, In: Oceanography of the
- 364 Mediterranean Sea, edited by: Schroeder, K., and Chiggiato, Jo., Elsevier, Amsterdam, pp. 387 -451,
- 365 <u>https://doi.org/10.1016/B978-0-12-823692-5.00004-2</u>, 2023.
- 366 Amorim, F. L. L., Le Meur, J., Wirth, A., and Cardin, V.: Tipping of the double-diffusive regime in the southern
- 367 Adriatic Pit in 2017 in connection with record high-salinity values, Ocean Sci., 20, 463-474,
- 368 <u>https://doi.org/10.5194/os-20-463-2024</u>, 2024.
- 369 Artegiani, A., Paschini, E., Russo, A., Bregant, D., Raicich, F., and Pinardi, N.: The Adriatic Sea General
- 370 Circulation. Part I: Air-Sea Interactions and Water Mass Structure, J. Phys. Oceanogr., 27, 1492-1514,
- 371 https://doi.org/10.1175/1520-0485(1997)027<1492:tasgcp>2.0.co;2, 1997.
- 372 Bensi, M.: THERMOHALINE VARIABILITY AND MESOSCALE DYNAMICS OBSERVED AT THE
- 373 E2M3A DEEP-SITE IN THE SOUTH ADRIATIC SEA, PhD thesis, Università degli studi di Trieste, Italy, 2012.





- 374 Bensi, M., Cardin, V., Rubino, A., Notarstefano, G., and Poulain, P. M.: Effects of winter convection on the deep
- 375 layer of the Southern Adriatic Sea in 2012: Effects of strong shelf convection, J. Geophys. Res. Oceans, 118,
- 376 6064–6075, https://doi.org/10.1002/2013jc009432, 2013.
- 377 Bensi, M., Cardin, V., and Rubino, A.: Thermohaline variability and mesoscale dynamics observed at the deep-
- 378 ocean observatory E2M3A in the southern Adriatic sea, in The Mediterranean Sea: Temporal Variability and
- 379 Spatial Patterns, Geophysical Monograph Series, eds G. L. E. Borzelli, M. Gačić, P. Lionello, and P. Malanotte-
- 380 Rizzoli (Oxford, UK: John Wiley & Sons, Inc.), 139–155, https://doi.org/10.1002/9781118847572.ch9, 2014
- 381 Bignami, F., Salusti, E., and Schiarini, S.: Observations on a bottom vein of dense water in the southern Adriatic
- 382 and Ionian seas, J. Geophys. Res., 95, 7249–7259, https://doi.org/10.1029/jc095ic05p07249, 1990.
- 383 Bozzano, R., Pensieri, S., Pensieri, L., Cardin, V., Brunetti, F., Bensi, M., Petihakis, G., Tsagaraki, T. M.,
- 384 Ntoumas, M., Podaras, D., and Perivoliotis, L.: The M3A network of open ocean observatories in the
- 385 Mediterranean Sea, in: 2013 MTS/IEEE OCEANS-Bergen, IEEE, Bergen, Norway, 10-14 June 2013, 1-10,
- 386 <u>https://doi.org/10.1109/OCEANS-Bergen.2013.6607996</u>, 2013.
- 387 Bunsen, F., Nissen, C., and Hauck, J.: The Impact of Recent Climate Change on the Global Ocean Carbon Sink,
- 388 Geophysical Research Letters, 51, https://doi.org/10.1029/2023g1107030, 2024.
- 389 Cantoni, C., Luchetta, A., Celio, M., Cozzi, S., Raicich, F., and Catalano, G.: Carbonate system variability in the
- 390 Gulf of Trieste (North Adriatic Sea), Estuarine, Coastal and Shelf Science, 115, 51-62,
- 391 https://doi.org/10.1016/j.ecss.2012.07.006, 2012.
- 392 Cantoni, C., De Vittor, C., Faganeli, J., Giani, M., Kovač, N., Malej, A., Ogrinc, N., Tamše, S., and Turk, V.:
- 393 Carbonate system and acidification of the Adriatic Sea, Marine Chemistry, 267, 104462,
- 394 <u>https://doi.org/10.1016/j.marchem.2024.104462</u>, 2024.
- 395 Cardin, V., Bensi, M., and Pacciaroni, M.: Variability of water mass properties in the last two decades in the South
- 396 Adriatic Sea with emphasis on the period 2006-2009, Continental Shelf Research, 31, 951-965,
- 397 https://doi.org/10.1016/j.csr.2011.03.002, 2011.
- 398 Cardin V., Siena, G., Giorgetti, A., Ursella, L., Brosich, A., and Partescano, E.: The Ritmare Fixed Sites Network
- 399 Procedures for Real-Time Data Quality Control, https://doi.org/10.13140/RG.2.2.31100.44166, 2014.
- 400 Cardin, V., Wirth, A., Khosravi, M., and Gačić, M.: South Adriatic Recipes: Estimating the Vertical Mixing in
- 401 the Deep Pit, Front. Mar. Sci., 7, https://doi.org/10.3389/fmars.2020.565982, 2020.
- 402 Cardin, V., Dentico, C., Brunetti, F., Bubbi, A., Chiaruttini, L., Civitarese, G., et al.: EMSO-E2M3A-B-Surface-
- time-series-South-Adriatic [dataset], https://doi.org/10.13120/y2hw-1j63, 2025.
- 404 Civitarese, G., Gačić, M., Batistić, M., Bensi, M., Cardin, V., Dulčić, J., Garić, R., and Menna, M.: The BiOS
- 405 mechanism: History, theory, implications, Progress in Oceanography, 216, 103056,
- 406 https://doi.org/10.1016/j.pocean.2023.103056, 2023.





- 407 Coppola, L., Ntoumas, M., Bozzano, R., Bensi, M., Hartman, S. E., Charcos Llorens, M., Craig, J., Rolin, J-F.,
- 408 Giovanetti, G., Cano, D., Karstensen, J., Cianca, A., Toma, D., Stasch, C., Pensieri, S., Cardin, V., Tengberg, A.,
- 409 Petihakis, G., and Cristini, L.: Handbook of Best Practices for Open Ocean Fixed Observatories, FixO3 Project,
- 410 127, FP7 Programme 2007–2013 under grant agreement no 312463, European Commission, 2016.
- 411 CO₂.Earth: http://co2.earth/, last access: 14 July 2025.
- 412 Dickson, A.G.: Therodynamics of the dissociation of boric acid and synthetic seawater from 273.15 to 318.15 K.
- 413 Deep -Sea Res. 137, 755 –766, 1990.
- 414 Dickson, A., Sabine, C., and Christian, J.R.: Guide to best practice for ocean CO 2 measurements. PICES Special
- 415 Pubbl. 3, 2007.
- 416 Fedele, G., Mauri, E., Notarstefano, G., and Poulain, P. M.: Characterization of the Atlantic Water and Levantine
- 417 Intermediate Water in the Mediterranean Sea using Argo Float Data. Ocean Science Discussions, 1-41,
- 418 <u>https://doi.org/10.5194/os-18-129-2022,</u> 2021.
- 419 Frangoulis, C., Stamataki, N., Pettas, M., Michelinakis, S., King, A. L., Giannoudi, L., Tsiaras, K., Christodoulaki,
- 420 S., Seppälä, J., Thyssen, M., Borges, A. V., and Krasakopoulou, E.: A carbonate system time series in the Eastern
- 421 Mediterranean Sea. Two years of high-frequency in-situ observations and remote sensing, Front. Mar. Sci., 11,
- 422 1348161, https://doi.org/10.3389/fmars.2024.1348161, 2024.
- Friederich, G. E., Brewer, P. G., Herlien, R., and Chavez, F. P.: Measurement of sea surface partial pressure of
- 424 CO2 from a moored buoy, Deep-Sea Res. Pt. I, 42, 1175–1186, https://doi.org/10.1016/0967-0637(95)00044-7,
- 425 1995
- 426 Friedlingstein, P., O'Sullivan, M., Jones, M. W., Andrew, R. M., Hauck, J., Landschützer, P., Le Quéré, C., Li,
- 427 H., Luijkx, I. T., Olsen, A., Peters, G. P., Peters, W., Pongratz, J., Schwingshackl, C., Sitch, S., Canadell, J. G.,
- 428 Ciais, P., Jackson, R. B., Alin, S. R., Arneth, A., Arora, V., Bates, N. R., Becker, M., Bellouin, N., Berghoff, C.
- 429 F., Bittig, H. C., Bopp, L., Cadule, P., Campbell, K., Chamberlain, M. A., Chandra, N., Chevallier, F., Chini, L.
- 430 P., Colligan, T., Decayeux, J., Djeutchouang, L., Dou, X., Duran Rojas, C., Enyo, K., Evans, W., Fay, A., Feely,
- 431 R. A., Ford, D. J., Foster, A., Gasser, T., Gehlen, M., Gkritzalis, T., Grassi, G., Gregor, L., Gruber, N., Gürses,
- 432 Ö., Harris, I., Hefner, M., Heinke, J., Hurtt, G. C., Iida, Y., Ilyina, T., Jacobson, A. R., Jain, A., Jarníková, T.,
- Jersild, A., Jiang, F., Jin, Z., Kato, E., Keeling, R. F., Klein Goldewijk, K., Knauer, J., Korsbakken, J. I., Lauvset,
- S. K., Lefèvre, N., Liu, Z., Liu, J., Ma, L., Maksyutov, S., Marland, G., Mayot, N., McGuire, P., Metzl, N.,
- 435 Monacci, N. M., Morgan, E. J., Nakaoka, S.-I., Neill, C., Niwa, Y., Nützel, T., Olivier, L., Ono, T., Palmer, P. I.,
- 436 Pierrot, D., Qin, Z., Resplandy, L., Roobaert, A., Rosan, T. M., Rödenbeck, C., Schwinger, J., Smallman, T. L.,
- 437 Smith, S., Sospedra-Alfonso, R., Steinhoff, T., Sun, Q., et al.: Global Carbon Budget 2024,
- 438 https://doi.org/10.5194/essd-2024-519, 13 November 2024.
- 439 Gačić, M., Marullo, S., Santoleri, R., and Bergamasco, A.: Analysis of the seasonal and interannual variability of
- 440 the sea surface temperature field in the Adriatic Sea from AVHRR data (1984-1992), J. Geophys. Res., 102,
- 441 22937–22946, https://doi.org/10.1029/97jc01720, 1997.





- 442 Gačić, M., Civitarese, G., Eusebi Borzelli, G. L., Kovačević, V., Poulain, P.-M., Theocharis, A., Menna, M.,
- 443 Catucci, A., and Zarokanellos, N.: On the relationship between the decadal oscillations of the northern Ionian Sea
- 444 and the salinity distributions in the eastern Mediterranean, J. Geophys. Res., 116,
- 445 https://doi.org/10.1029/2011jc007280, 2011.
- 446 García-Ibáñez, M. I., Guallart, E. F., Lucas, A., Pascual, J., Gasol, J. M., Marrasé, C., Calvo, E., and Pelejero, C.:
- 447 Two new coastal time-series of seawater carbonate system variables in the NW Mediterranean Sea: rates and
- 448 mechanisms controlling pH changes, Front. Mar. Sci., 11, https://doi.org/10.3389/fmars.2024.1348133, 2024.
- 449 Gattuso, J-P, and Hansson L. (Eds). Ocean acidification. Oxford university press, 2011.
- 450 Hassoun, A. E. R., Gemayel, E., Krasakopoulou, E., Goyet, C., Abboud-Abi Saab, M., Guglielmi, V., Touratier,
- 451 F., and Falco, C.: Acidification of the Mediterranean Sea from anthropogenic carbon penetration, Deep Sea
- 452 Research Part I: Oceanographic Research Papers, 102, 1–15, https://doi.org/10.1016/j.dsr.2015.04.005, 2015.
- 453 Hassoun, A. E. R., Bantelman, A., Canu, D., Comeau, S., Galdies, C., Gattuso, J.-P., Giani, M., Grelaud, M.,
- 454 Hendriks, I. E., Ibello, V., Idrissi, M., Krasakopoulou, E., Shaltout, N., Solidoro, C., Swarzenski, P. W., and
- 455 Ziveri, P.: Ocean acidification research in the Mediterranean Sea: Status, trends and next steps, Front. Mar. Sci.,
- 456 9, https://doi.org/10.3389/fmars.2022.892670, 2022.
- 457 ICOS-Ocean Thematic Center: https://www.icos-otc.org/, last access: 14 October 2025.
- 458 Intergovernmental Panel on Climate Change (IPCC). Changing State of the Climate System. In: Climate Change
- 459 2021 The Physical Science Basis: Working Group I Contribution to the Sixth Assessment Report of the
- 460 Intergovernmental Panel on Climate Change. Cambridge University Press; 2023:287-422, 2021.
- 461 Ingrosso, G., Giani, M., Comici, C., Kralj, M., Piacentino, S., De Vittor, C., and Del Negro, P.: Drivers of the
- 462 carbonate system seasonal variations in a Mediterranean gulf, Estuarine, Coastal and Shelf Science, 168, 58–70,
- 463 <u>https://doi.org/10.1016/j.ecss.2015.11.001</u>, 2016.
- 464 Ingrosso, G., Bensi, M., Cardin, V., and Giani, M.: Anthropogenic CO2 in a dense water formation area of the
- 465 Mediterranean Sea, Deep Sea Research Part I: Oceanographic Research Papers, 123, 118-128,
- 466 <u>https://doi.org/10.1016/j.dsr.2017.04.004</u>, 2017...
- 467 IOC UNESCO: https://www.ioc.unesco.org/en, last access: 21 July 2025.
- 468 Kapsenberg, L., Alliouane, S., Gazeau, F., Mousseau, L., and Gattuso, J.-P.: Concomitant ocean acidification and
- 469 increasing total alkalinity at a coastal site in the NW Mediterranean Sea (2007-2015), https://doi.org/10.5194/os-
- 470 <u>2016-71</u>, 13 September 2016.
- 471 Lee, K., Kim, T.-W., Byrne, R.H., Millero, F.J., Feely, R.A., Liu, Y.-M.: The universal ratio of boron to chlorinity
- 472 for the North Pacific and North Atlantic oceans. Geochim. Cosmochim. Acta 74, 1801 –1811, 2010.





- 473 Lueker, T. J., Dickson, A. G., and Keeling, C. D.: Ocean pCO 2 calculated from dissolved inorganic carbon,
- 474 alkalinity, and equations for K1 and K2: Validation based on laboratory measurements of CO 2 in gas and seawater
- 475 at equilibrium. Mar. Chem. 70, 105 –119, 2000.
- 476 Le Meur, J., Wirth, A., Paladini De Mendoza, F., Miserocchi, S., and Cardin, V.: Intermittent supply of dense
- 477 water to the deep South Adriatic Pit: an observational study, Front. Mar. Sci., 12,
- 478 https://doi.org/10.3389/fmars.2025.1516780, 2025.
- 479 Malanotte-Rizzoli, P.: The Northern Adriatic Sea as a prototype of convection and water mass formation on the
- 480 continental shelf P.C Chu, J.C Gascard (Eds.), Deep Convection and Deep Water Formation in the Oceans,
- 481 Elsevier Oceanography Series, vol. 57, Elsevier, Amsterdam, pp. 229-239, 1991.
- 482 Martellucci, R., Giani, M., Mauri, E., Coppola, L., Paulsen, M., Fourrier, M., Pensieri, S., Cardin, V., Dentico,
- 483 C., Bozzano, R., Cantoni, C., Lucchetta, A., Izquierdo, A., Bruno, M., and Skjelvan, I.: CO₂ and hydrography
- 484 acquired by autonomous surface vehicles from the Atlantic Ocean to the Mediterranean Sea: data correction and
- validation, Earth Syst. Sci. Data, 16, 5333–5356, https://doi.org/10.5194/essd-16-5333-2024, 2024a.
- 486 Martellucci, R., Menna, M., Mauri, E., Pirro, A., Gerin, R., Paladini De Mendoza, F., Garić, R., Batistić, M., Di
- 487 Biagio, V., Giordano, P., Langone, L., Miserocchi, S., Gallo, A., Notarstefano, G., Savonitto, G., Bussani, A.,
- 488 Pacciaroni, M., Zuppelli, P., and Poulain, P.-M.: Recent changes of the dissolved oxygen distribution in the deep
- 489 convection cell of the southern Adriatic Sea, Journal of Marine Systems, 245, 103988,
- 490 <u>https://doi.org/10.1016/j.jmarsys.2024.103988</u>, 2024b.
- 491 Martellucci, R., Dentico, C., Coppola, L., Skjelvan, I., Giani, M., Pensieri, S., Cantoni, C., Cardin, V., Fourrier,
- 492 M., Bozzano, R., Paulsen, M., and Mauri, E.: Air-sea CO2 exchange in the Eastern Atlantic and the Mediterranean
- Sea based on autonomous surface measurements, 2025. In review.
- 494 Menna, M., Martellucci, R., Notarstefano, G., Mauri, E., Gerin, R., Pacciaroni, M., et al.: Record-breaking high
- 495 salinity in the South Adriatic Pit in 2020, in: Copernicus Ocean State Report, issue 6. Journal of Operational
- 496 Oceanography, 15(sup1), 1–220. https://doi.org/10.1080/1755876X.2022.2095169, 2022.
- 497 Mihanović, H., Vilibić, I., Šepić, J., Matić, F., Ljubešić, Z., Mauri, E., Gerin, R., Notarstefano, G., and Poulain,
- 498 P.-M.: Observation, Preconditioning and Recurrence of Exceptionally High Salinities in the Adriatic Sea, Front.
- 499 Mar. Sci., 8, 672210, https://doi.org/10.3389/fmars.2021.672210, 2021.
- 500 Ovchinnikov, I.M., Zats, V.I., Krivosheya, V.G., and Udodov, A.I.: Formation of deep Eastern Mediterranean
- 501 waters in the Adriatic Sea. Oceanology, 25, 6, 704-707, 1985.
- 502 Orr, J. C., Epitalon, J.-M., and Gattuso, J.-P.: Comparison of ten packages that compute ocean carbonate
- 503 chemistry, Biogeosciences, 12, 1483–1510, https://doi.org/10.5194/bg-12-1483-2015, 2015.
- 504 Oudot, C., Gerard, R., Morin, P.: Precise shipboard determination of dissolved oxygen (Winkler procedure) for
- productivity studies with commercial system. Limnology and Oceanography 33, 146e150, 1988.





- 506 Pecci, M., Sferlazzo, D., Anello, F., Becagli, S., Colella, S., Silvestri, L. D., Iorio, T. D., Meloni, D., Monteleone,
- 507 F., Piacentino, S., Principato, E., and Sarra, A. D.: Large influence of the 2022-23 marine heatwave on the air-sea
- 508 CO2 flux in the Central Mediterranean, https://doi.org/10.22541/essoar.173393985.55347710/v1, 11 December
- 509 2024.
- 510 Pierrot, D., Lewis, E., and Wallace, D. W. R.: MS Excel Program Developed for CO2 system calculations.
- 511 https://cdiac.ess -drive.lbl.cov/ftp/co2sys/CO2SYS_calc_XLS_v2.1/, 2006.
- 512 Ravaioli, M., Bergami, C., Riminucci, F., Langone, L., Cardin, V., Di Sarra, A., Aracri, S., Bastianini, M., Bensi,
- 513 M., Bergamasco, A., Bommarito, C., Borghini, M., Bortoluzzi, G., Bozzano, R., Cantoni, C., Chiggiato, J., Crisafi,
- 514 E., D'Adamo, R., Durante, S., Fanara, C., Grilli, F., Lipizer, M., Marini, M., Miserocchi, S., Paschini, E., Penna,
- 515 P., Pensieri, S., Pugnetti, A., Raicich, F., Schroeder, K., Siena, G., Specchiulli, A., Stanghellini, G., Vetrano, A.,
- 516 and Crise, A.: The RITMARE Italian Fixed-Point Observatory Network (IFON) for marine environmental
- 517 monitoring: a case study, Journal of Operational Oceanography, 9, s202-s214,
- 518 https://doi.org/10.1080/1755876x.2015.1114806, 2016.
- 519 Riebesell, U., Gattuso, J. P., Thingstad, T. F., & Middelburg, J. J.:. Arctic ocean acidification: pelagic ecosystem
- 520 and biogeochemical responses during a mesocosm study. Biogeosciences, 10, 5619-5626, doi:10.5194/bg-10-
- **521** 5619-2013, 2013.
- 522 Robinson, A.R., Leslie, W.G., Theocharis, A., and Lascaratos, A.: Mediterranean Sea circulation. Encyclopedia
- 523 of Ocean Sciences Academic Press, Harcourt Science & Technology, Harcourt Place, 32 Jamestown Road London
- 524 NW1 7BY UK, pp. 1689–1705, 2001.
- 525 Roether, W. and Schlitzer, R.: Eastern Mediterranean deep water renewal on the basis of chlorofluoromethane
- 526 and tritium data, Dynamics of Atmospheres and Oceans, 15, 333-354, https://doi.org/10.1016/0377-
- 527 <u>0265(91)90025-b</u>, 1991.
- 528 Schlitzer, R., Roether, W., Oster, H., Junghans, H.-G., Hausmann, M., Johannsen, H., and Michelato, A.:
- 529 Chlorofluoromethane and oxygen in the Eastern Mediterranean, Deep Sea Research Part A. Oceanographic
- 530 Research Papers, 38, 1531–1551, https://doi.org/10.1016/0198-0149(91)90088-w, 1991.
- 531 Schneider, A., Tanhua, T., Körtzinger, A., and Wallace, D. W. R.: High anthropogenic carbon content in the
- eastern Mediterranean, J. Geophys. Res., 115, https://doi.org/10.1029/2010jc006171, 2010.
- 533 Schroeder, K., Ben Ismail, S., Bensi, M., Bosse, A., Chiggiato, J., Civitarese, G., Falcieri M, F., Fusco, G., Gačić,
- 534 M., Gertman, I., Kubin, E., Malanotte-Rizzoli, P., Martellucci, R., Menna, M., Ozer, T., Taupier-Letage, I.,
- 535 Vargas-Yáñez, M., Velaoras, D., and Vilibić, I.: A consensus-based, revised and comprehensive catalogue for
- 536 Mediterranean water masses acronyms. Mediterranean Marine Science, 25(3), 783-791.
- 537 https://doi.org/10.12681/mms.38736, 2024.
- 538 Steinhoff, T., Gkritzalis, T., Jones, S., Macovei, V. A., Neill, C., Schuster, U., Akl, J., Arruda, R., Atamanchuk,
- 539 D., Barry, M., Beaumont, L., Cantoni, C., Dickson, A., Fahning, J., Fought, J., Frangoulis, C., Gutiérrez-Loza, L.,
- Hagan, C., Honkanen, M., Kielosto, S., Kinski, N., Körtzinger, A., Landschützer, P., Lauvset, S. K., Lawrence-

© Author(s) 2025. CC BY 4.0 License.





- 541 Slavas, N., Li, Q., Luchetta, A., Malarde, D., Paulsen, M., Ritschel, M., Rutgersson, A., Sanders, R., Shitashima,
- 542 K., Spaulding, R., Stamataki, N., Stenbäck, K., Sutton, A., Tatkiewicz, W., Telszewski, M., Theetaert, H.,
- 543 Tilbrook, B., and Wanninkhof, R.: The ICOS OTC PCO2 instrument intercomparison, Limnology & Tilbrook, B., and Wanninkhof, R.: The ICOS OTC PCO2 instrument intercomparison, Limnology & Tilbrook, B., and Wanninkhof, R.: The ICOS OTC PCO2 instrument intercomparison, Limnology & Tilbrook, B., and Wanninkhof, R.: The ICOS OTC PCO2 instrument intercomparison, Limnology & Tilbrook, B., and Wanninkhof, R.: The ICOS OTC PCO2 instrument intercomparison, Limnology & Tilbrook, B., and Wanninkhof, R.: The ICOS OTC PCO2 instrument intercomparison, Limnology & Tilbrook, B., and Wanninkhof, R.: The ICOS OTC PCO2 instrument intercomparison, Limnology & Tilbrook, B., and Wanninkhof, R.: The ICOS OTC PCO2 instrument intercomparison, Limnology & Tilbrook, B., and Wanninkhof, R.: The ICOS OTC PCO2 instrument intercomparison, Limnology & Tilbrook, B., and the ICOS OTC PCO2 instrument intercomparison, Limnology & Tilbrook, B., and the ICOS OTC PCO2 instrument intercomparison, Limnology & Tilbrook, B., and the ICOS OTC PCO2 instrument intercomparison, Limnology & Tilbrook, B., and the ICOS OTC PCO2 instrument intercomparison, Limnology & Tilbrook, B., and the ICOS OTC PCO2 instrument intercomparison, Limnology & Tilbrook, B., and the ICOS OTC PCO2 instrument intercomparison, Limnology & Tilbrook, B., and the ICOS OTC PCO2 instrument intercomparison, Limnology & Tilbrook, B., and the ICOS OTC PCO2 instrument intercomparison, Limnology & Tilbrook, B., and the ICOS OTC PCO2 instrument intercomparison, Limnology & Tilbrook, B., and the ICOS OTC PCO2 instrument intercomparison, Limnology & Tilbrook, B., and the ICOS OTC PCO2 instrument intercomparison, Limnology & Tilbrook, B., and the ICOS OTC PCO2 instrument intercomparison, Limnology & Tilbrook, B., and the ICOS OTC PCO2 instrument intercomparison, Limnology & Tilbrook, B., and the ICOS OTC PCO2 instrument intercomparison, Limnology & Tilbrook, B., and the ICOS OTC PCO2 instrument intercomparison, Limnology & Tilbrook, B., and the ICOS OTC PCO2 instrument intercomparison, Limnology
- 544 Methods, lom3.10727, https://doi.org/10.1002/lom3.10727, 2025.
- Taillandier, V., D'Ortenzio, F., Prieur, L., Conan, P., Coppola, L., Cornec M., Dumas F., Durrieu de Madron X.,
- Fach B., Fourrier M., Gentil M., Hayes D., Husrevoglu S., Legoff H., Le Sterl L., Örek H., Ozer T., Poulain P.
- 547 M., Pujo-Pay M., Ribera d'Alcalà M., Salihoglu B., Testor P., Velaoras D., Wagener T., and Wimart-Rousseauet
- 548 C.: Sources of the Levantine intermediate water in winter 2019. Journal of Geophysical Research: Oceans, 127,
- 549 https://doi.org/10.1029/2021JC017506, 2022.
- 550 Takahashi, T., Olafsson, J., Goddard, J. G., Chipman, D. W., and Sutherland, S. C.: Seasonal variation of CO₂
- and nutrients in the high-latitude surface oceans: A comparative study, Global Biogeochemical Cycles, 7, 843–
- 552 878, https://doi.org/10.1029/93GB02263, 1993.
- Takahashi, T., Sutherland, S. C., Wanninkhof, R., Sweeney, C., Feely, R. A., Chipman, D. W., Hales, B.,
- 554 Friederich, G., Chavez, F., Sabine, C., Watson, A., Bakker, D. C. E., Schuster, U., Metzl, N., Yoshikawa-Inoue,
- 555 H., Ishii, M., Midorikawa, T., Nojiri, Y., Körtzinger, A., Steinhoff, T., Hoppema, M., Olafsson, J., Arnarson, T.
- 556 S., Tilbrook, B., Johannessen, T., Olsen, A., Bellerby, R., Wong, C. S., Delille, B., Bates, N. R., and De Baar, H.
- 557 J. W.: Climatological mean and decadal change in surface ocean pCO2, and net sea-air CO2 flux over the global
- 558 oceans, Deep Sea Research Part II: Topical Studies in Oceanography, 56, 554-577,
- 559 <u>https://doi.org/10.1016/j.dsr2.2008.12.009</u>, 2009.
- The MathWorks Inc. MATLAB version: 9.13.0 (R2023b), Natick, Massachusetts: The MathWorks Inc.
- 561 https://www.mathworks.com, 2022.
- 562 Touratier, F. and Goyet, C.: Impact of the Eastern Mediterranean Transient on the distribution of anthropogenic
- 563 CO2 and first estimate of acidification for the Mediterranean Sea, Deep Sea Research Part I: Oceanographic
- Research Papers, 58, 1–15, https://doi.org/10.1016/j.dsr.2010.10.002, 2011.
- 565 Turk, D., Malačič, V., DeGrandpre, M. D., and McGillis, W. R.: Carbon dioxide variability and air-sea fluxes in
- the northern Adriatic Sea, J. Geophys. Res., 115, 2009JC006034, https://doi.org/10.1029/2009JC006034, 2010.
- 567 Urbini, L., Ingrosso, G., Djakovac, T., Piacentino, S., and Giani, M.: Temporal and Spatial Variability of the CO2
- 568 System in a Riverine Influenced Area of the Mediterranean Sea, the Northern Adriatic, Front. Mar. Sci., 7,
- 569 https://doi.org/10.3389/fmars.2020.00679, 2020.
- 570 Vilibić, I. and Orlić, M.: Least-squares tracer analysis of water masses in the South Adriatic (1967–1990), Deep
- 571 Sea Research Part I: Oceanographic Research Papers, 48, 2297-2330, https://doi.org/10.1016/s0967-
- 572 <u>0637(01)00014-0</u>, 2001.